JOURNAL OF Applied Polymer SCIENCE

Preparation and Characterization of a Poly(vinyl alcohol)/Tetraethoxysilane Ultrafiltration Membrane by a Sol-Gel Method

Haikuan Yuan,[1,2] Jie Ren,[1,2] Liang Cheng,[3] Lian Shen[1,2]

[1]College of Chemical Engineering and Materials Science, Zhejiang University of Technology, Hangzhou 310014, China
[2]Zhejiang Province Key Laboratory of Biomass Fuel, Zhejiang University of Technology, Hangzhou 310014, China
[3]Chemical Engineering Research Center, East China University of Science and Technology, Shanghai 200237, China
Correspondence to: H. Yuan (E-mail: yhk12345@163.com)

ABSTRACT: Using poly(vinyl alcohol) (PVA) with highly hydrophilic properties as membrane material and poly(ethylene glycol) (PEG) as an additive, we prepared PVA/tetraethoxysilane (TEOS) ultrafiltration (UF) membranes with good antifouling properties by a sol–gel method. The PVA/TEOS UF membranes were characterized by X-ray diffraction patterns, Fourier transform infrared spectroscopy, scanning electron microscopy, and static contact angle of measurement of water. The hybridization of TEOS to PVA for preparing the PVA/TEOS UF membranes achieved the required permeation performance and good antifouling behaviors. The morphology and permeation performance of the PVA/TEOS membranes varied with the different TEOS loadings and PEG contents. The pure water fluxes (J_W) increased and the rejections (Rs) decreased with increasing TEOS loading and PEG content. The PVA/TEOS UF membrane with a PVA/TEOS/PEG/H_2O composition mass ratio of 10/3/4/83 in the dope solution had a J_W of 66.5 L m^{-2} h^{-1} and an R of 60.3% when we filtered it with 300 ppm of bovine serum albumin aqueous solution at an operational pressure difference of 0.1 MPa. In addition, the filtration and backwashing experiment proved that the PVA/TEOS membranes possessed good long-term antifouling abilities. © 2013 Wiley Periodicals, Inc. J. Appl. Polym. Sci. 130: 4066–4074, 2013

KEYWORDS: hydrophilic polymers; membranes; morphology; properties and characterization; separation techniques

Received 24 October 2012; accepted 4 May 2013; Published online 8 July 2013
DOI: 10.1002/app.39502

INTRODUCTION

Ultrafiltration (UF) membranes have been widely used in many industrial separation processes, including wastewater treatment, reverse osmosis pretreatment, and the separation of solutes in chemical, pharmaceutical, and beverage industries.[1–3] However, one major problem for the application of UF membranes is fouling, which results in decreases in the flux and separation abilities of the membrane.[4] Research on the reduction of membrane fouling and the preparation of antifouling membranes has gained increasing attention in recent years. The hydrophilicity of the membrane plays important role in membrane separation processes, especially for the antifouling properties. Lots of modifications to UF membranes with high antifouling properties have been studied through physical and chemical methods, mostly on the endowment of a hydrophobic membrane with hydrophilic properties,[5,6] blending,[7] or grafting with hydrophilic monomers.[8,9] The use of hydrophilic materials, that is, poly(vinyl alcohol) (PVA), to modify the hydrophobic membrane surface is a very interesting way to improve the hydrophilicity of the membrane and the antifouling properties. Recently, a unique class of thin-film nanofibrous composite UF membranes based on the coating of a PVA hydrogel barrier layer on a nanofibrous layer were demonstrated; these membranes exhibited a high flux, high rejection (R), and good antifouling properties; however, electrospinning or electrospraying techniques were used, and it was also difficult to ensure a homogeneous thinner barrier layer.[10–12]

Another effective approach to reducing fouling is the use of hydrophilic polymers to prepare UF membranes, which exhibit a greater fouling resistance to protein than hydrophobic membranes.[13,14] PVA, with its highly hydrophilic characteristics, good film-forming properties, and outstanding biocompatibility, is an excellent membrane material for the preparation of a hydrophilic membrane.[15,16] Although considerable studies of PVA material have been done for reverse osmosis, pervaporation, and nanofiltration membranes,[17–20] studies on the preparation of PVA UF membranes are relatively rare.[21,22] The chemical constitution and solubility of PVA infer the disadvantages of easier degradation and elimination after use; this has been a barrier for its application in the UF field. Many studies have been attempted to improve the stability and the mechanical properties of PVA membranes by chemical crosslinking,[16,23]

heat treatment,[23] grafting,[24] interfacial polymerization,[25,26] and organic–inorganic hybridization.[27] Among these methods, hybridization is of the greatest interest; a hybrid membrane would promise to complement and optimize the properties of organic and inorganic materials. Therefore, hybridization is a good way to improve the chemical, mechanical, and thermal properties of organic materials.[28,29] If PVA material is used to prepare UF membranes, an important step is to improve its poor wet strength and the permeation performance; this could be solved by organic–inorganic hybridization to PVA. Inorganic materials are embedded in the PVA matrix strongly through the covalent bonds with the hydroxyl groups in PVA; this improves the mechanical strength and depresses the water solubility of the membrane. Meanwhile, the hybrid PVA membrane retains a strong hydrophilicity; consequently, it shows the good antifouling properties. Jiang and Wang[30,31] once prepared nanosized silica/PVA composite UF membranes with a high mechanical strength and good antifouling properties; in there experiment, the *ex situ* generated silica was used to hybridize the PVA material. However, the homogeneity of the SiO_2 particles in the PVA matrix could not be assured because there were no strong covalent bonds to form the crosslinking frameworks between the PVA and SiO_2 particles. If the hybrid were prepared by PVA and a metal alkoxide, such as tetraethoxysilane (TEOS), through the sol–gel technique, which would involve the hydrolysis and condensation of TEOS, crosslinking frameworks under mild conditions and the homogeneous incorporation of minerals into PVA membrane with the increased properties would be formed.

In this study, PVA/TEOS UF membranes were prepared by the sol–gel method. The characterization and properties of the membranes, including the microstructure, morphology, permeation performance, and antifouling properties, are fully discussed.

EXPERIMENTAL

Chemicals

PVA with a polymerization degree of 1750 ± 50 and an alcoholysis degree of 98% was purchased from Sinopharm Chemical Reagent Co., Ltd. (Shanghai, China). Poly(ethylene glycol) (PEG) with a molecular weight of 1000 was purchased from Pudong Gaonan Chemical Plant (Shanghai, China). TEOS was obtained from Wulian Chemical Plant (Shanghai, China); Hydrochloric acid (HCl, 36–38%) was purchased from Reagent Co., Ltd., of Juhua Group Corp. (Quzhou, China). The sodium hydroxide (NaOH) was from Xiaoshan Chemical Reagent Co., Ltd. (Hangzhou, China), and anhydrous sodium sulfate (Na_2SO_4) was from Shisihewei Chemical Co., Ltd. (Shanghai, China). Bovine serum albumin (BSA; weight-average molecular weight = 67,000) was purchased from Xueman Biology Sci and Tech Co., Ltd. (Shanghai, China). The deionized water was self-made in the laboratory. All chemicals were analytical grade and were used as received without further purification.

Preparation of the PVA/TEOS UF Membranes

The PVA/TEOS UF membranes were prepared by the sol–gel reaction of PVA and TEOS with the phase-inversion method. First, 6.9 mL (0.3822 mol) of deionized water, 0.1 mL of hydrochloric acid (HCl; 1 mol/L), and 20 mL (0.0899 mol) of TEOS were mixed and stirred continuously for 3 h at room temperature until a uniform and stable TEOS sol was obtained. Second, prescribed amounts of PVA and PEG were solved in water at 95°C for 6 h to get a transparent solution. The TEOS sol was then added to the PVA and PEG mixed aqueous solution with constant stirring at room temperature for 1 h to get a homogeneous dope solution and was then degassed for 0.5 h. The dope solution was coated uniformly on a glass plate; then, the glass was immersed in a $Na_2SO_4/KOH/H_2O$ (saturated/75 g/1000 mL) coagulation bath for 0.5 h; thus, the PVA/TEOS UF membrane with a thickness of about 50–80 μm was prepared. After taking out the membrane from the coagulation bath, we kept in the water bath for 24 h and then transferred it to a 30 wt % glycerol aqueous solution to prevent the collapse of the porous membrane structure. The compositions of the PVA/TEOS dope solutions are listed in Table I.

Table I. Dope Composition for the Preparation of the PVA/TEOS UF Membranes

Membrane no.	PVA/PEG (mass ratio, wt %)	TEOS loading (wt %)	Thickness (μm)[a]
M1	10/4	0	68
M2	10/4	1	55
M3	10/4	2	65
M4	10/4	3	67
M5	10/4	4	70
M6	10/1.33	3	—
M7	10/2.67	3	—
M8	10/5.33	3	—
M9	10/6.67	3	—

[a] The average thickness for calculating the mean pore size of the membrane used in Table II.

Characterizations of the Membrane

X-ray Diffraction (XRD) and Fourier Transform Infrared (FTIR) Analysis. The XRD patterns of the PVA/TEOS membranes were recorded on a X'Pert PRO X-ray diffractometer (PANalytical, Holland) equipped with graphite monochromated Cu Kα radiation ($\lambda = 0.154056$ nm) operating at 40 mA and 40 kV from 5 to 60°.

The microstructure of the PVA/TEOS membrane was determined with an FTIR spectrometer equipped with attenuated total reflection crystals (Nicolet 6700), with scanning in the wave-number range of 4000–400 cm^{-1}.

Hydrophilicity Measurement. The static contact angles of the PVA/TEOS membranes were measured to quantify the change in hydrophilicity through the sessile drop method with a contact angle goniometer (JC2000D3, Shanghai Zhongchen Digital Equipment Co., Ltd., China). An ultrapure water drop (2-μL sampling for 10 s) was added by a microsyringe to a dry sample surface in an ambient atmosphere and at ambient humidity, and then, the contact angle was measured. The data represented an average of five measurements performed at different positions on the sample.

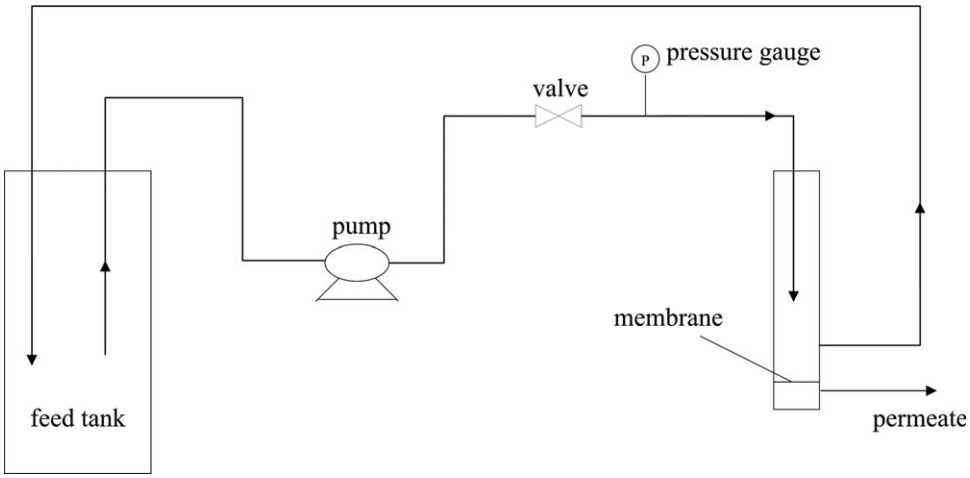

Figure 1. Schematic diagram for the UF experimental setup.

Porosity (ε; %) and Pore Size Measurements

The membrane ε is defined as the volume of the pores divided by the total volume of the porous membrane. It can usually be determined by the gravimetric method, depending on the weight of the liquid (pure water here) contained in the membrane pores.[32,33] To reduce the measurement errors, especially for the weight of the wet membrane (w_1), five wet parts and the corresponding dry ones of the same sample were measured, and the average value were obtained.

$$\varepsilon = \frac{(w_1 - w_2)/d_w}{(w_1 - w_2)/d_w + w_2/d_P} \times 100\% \quad (1)$$

where w_2 is the weight of the dry membrane (g), respectively, d_W is the pure water density (0.998 g cm^{-3}) and d_P is the membrane density (because the inorganic content in the membrane matrix is very small, d_P is approximate to that of PVA material, namely, 1.290 g cm^{-3}).

Mean pore radius [r_m (μm)] is determined by the filtration velocity method. According to Guerout–Elford–Ferry equation,[34] r_m could be calculated as follows:

$$r_m = \sqrt{\frac{(2.9 - 1.75\varepsilon) \times 8\eta l Q}{\varepsilon \times A \times \Delta P}}. \quad (2)$$

where η is the water viscosity (8.9 $\times$ 10^{-4} Pa s), l is the membrane thickness (m), Q is the volume of the permeate water per unit time (m^3 s^{-1}), A is the effective area of the membrane (m^2), and ΔP is the operational pressure difference (0.1 MPa).

Morphological Observation. The morphology of the PVA/TEOS membrane was observed by scanning electron microscopy (SEM; Hitachi S-4700, Japan). Before observing the cross-sectional morphology of membrane, we first immersed the sample into liquid nitrogen for a few minutes and then broke and deposited it onto a copper holder. All of the samples were coated with gold *in vacuo* before observation.

Permeation Performance of the Membranes

The permeation flux (J) and R of the membrane were measured through a UF experimental setup, as presented in Figure 1. The membrane was cut in a circle and installed in a cup-type ultrafilter (self-made); then, the measurement pressure was adjusted to the predetermined value through diaphragm pump. The effective area of the membrane for UF experiment was 7.06 cm^2. All of the experiments were conducted at room temperature and under an operational pressure difference of 0.1 MPa. The fresh membrane was prepressured at 0.1 MPa with pure water for 1 h; then the pure water flux (J_W) was measured. Finally, R of the membrane with 300 ppm of BSA aqueous solution was measured. The BSA concentrations in the permeate and the feed were determined by an ultraviolet–visible spectrophotometer (Ultrospec 1100 Pro). J and R were defined as follows, respectively:

$$J = \frac{V}{At}. \quad (3)$$

$$R = \left(1 - \frac{C_P}{C_F}\right) \times 100\% \quad (4)$$

where V is the permeation volume (L), A is the permeation area (m^2), t is the permeation time (s), and C_P and C_F are the BSA concentrations in the permeate and the feed, respectively.

Antifouling Properties of the Membranes

The flux recovery ratio (R_r) was used to evaluate the antifouling properties of the PVA/TEOS UF membranes. The membrane was first prepressured for 1 h with pure water at 0.1 MPa, and the pure water flux (J_{W1}) was measured. Then, 1000 ppm of the BSA aqueous solution was used to permeate through the membrane for 1 h. Afterward, the membrane was backwashed by pure water for 1 h, and then, the pure water flux (J_{W2}) was measured. The same membrane was filtered with the BSA aqueous solution and backwashed with water again, and the pure water fluxes (J_{W3} and J_{W4}) were measured in this cycle. R_r of membrane was calculated as follows:

$$(R_r)_{n/1} = \frac{J_{Wn}}{J_{W1}} \times 100\% \quad (5)$$

where $n = 2$, 3, and 4 and J_{W1} and J_{Wn} are the water flux for the fresh and cleaned membranes, respectively.

RESULTS AND DISCUSSION

XRD Analysis

XRD analysis was performed to examine the crystallinity of the PVA/TEOS membranes. It is well known that the PVA polymer exhibits a semicrystalline structure with a large peak at about 20°.[35,36] Figure 2 shows the XRD patterns of the PVA/TEOS membranes with different TEOS loadings. As shown in Figure 2, one peak appeared around a 2θ of 20° for the PVA/TEOS membranes, and the peak intensity decreased gradually with increasing TEOS loading. This indicated that the PVA/TEOS membranes became more amorphous with the introduction of TEOS; that is, the crystallinity of the membrane decreased. This was due to the occurrence of a crosslinking reaction between the hydroxyl groups of PVA and the silanol groups of the TEOS sol, which formed the Si—O—C bonds between the linear polyethylene segments.[37,38] As a result, the formation of a crystalline region between the PVA chains was restrained.

FTIR Spectra

The FTIR spectra of the PVA/TEOS membranes with different TEOS loadings are shown in Figure 3. The major vibration bands (Si—O—C at 1090 cm^{-1} and Si—OH at 950 cm^{-1}) associated with the hydrolysis and condensation of TEOS[39] and the crosslinking reaction between TEOS and PVA were observed, as shown in Figure 3. Similar to the FTIR spectrum of PVA, the peak ranging from 3650 to 3000 cm^{-1} for the PVA/TEOS hybrid membrane mainly corresponded to the hydroxyl groups. Its intensity decreased marginally after the introduction of TEOS into PVA; this indicated the decline of hydroxyl groups because of the crosslinking reaction between PVA and TEOS.

An important absorption peak in the PVA material was verified at a wave number of 1141 cm^{-1}; its intensity was influenced by the crystalline portion of the polymeric chains, and it was used to assess the crystallinity of PVA.[40,41] The absorbance ratio of a functional group (C—O) to a reference peak was calculated to analyze the structural changes of PVA quantitatively or half-quantitatively. The introduction of Si—OH and Si—O—Si

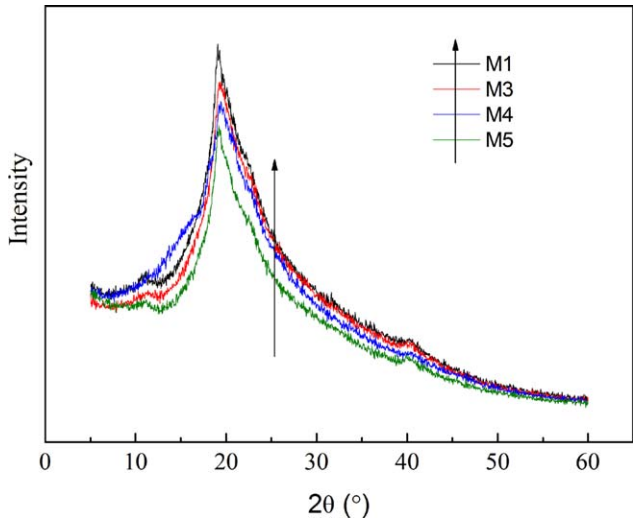

Figure 2. XRD patterns of the PVA/TEOS membranes. [Color figure can be viewed in the online issue, which is available at wileyonlinelibrary.com.]

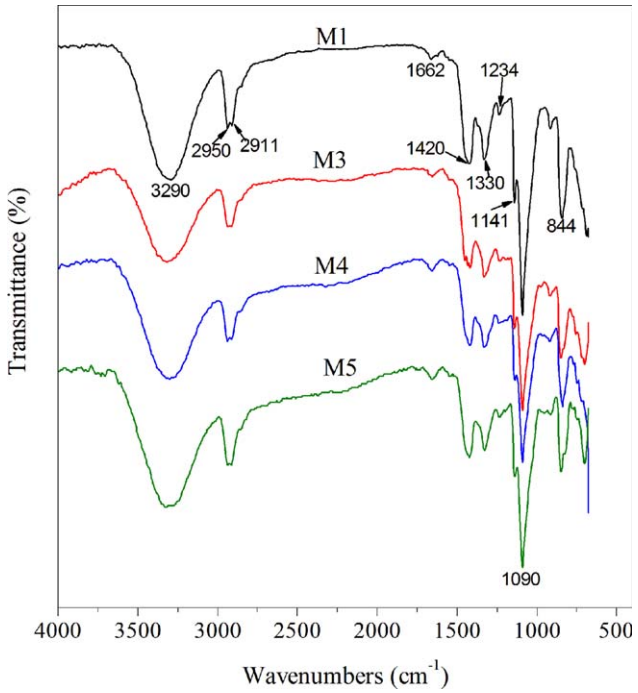

Figure 3. FTIR spectra of the PVA/TEOS membranes. [Color figure can be viewed in the online issue, which is available at wileyonlinelibrary.com.]

groups through the hydrolysis and condensation reactions of TEOS modified the initial semicrystalline structure of PVA. The peak at 1141 cm^{-1} for PVA was crystallinity-sensitive, whereas the peak at 1420 cm^{-1} was quite stable, so the height of these two peaks (h_{1420} and h_{1141}) could be used to calculate the crystallinity (X) of PVA as follows:[42,43]

$$X(\%) = a \times \frac{h_{1420}}{h_{1141}} - b. \quad (6)$$

where a and b are constants, where $a = 102.6$ and $b = 63.6$.

The crystallinities for M1, M3, M4, and M5 membranes calculated from eq. (6) were 39.81, 39.78, 39.53, and 38.07, respectively. Therefore, the calculated crystallinities of the PVA/TEOS membranes decreased with increasing TEOS loading; this corresponded with the analysis results from their XRD patterns.

Hydrophilicity and ε Values of the Membranes

The surface hydrophilicity could affect the J values and antifouling properties of the membranes, and it is generally evaluated by the measurement of the water contact angle on the membrane surface. A smaller water contact angle indicates a stronger hydrophilicity of the membrane surface.[44] The water contact angles of the PVA/TEOS membranes with different TEOS loadings are shown in Figure 4. As shown in Figure 4, the surface hydrophilicity of PVA/TEOS membrane decreased first and then increased with the TEOS loading. Although the amounts of hydroxyl groups generated from TEOS hydrolysis were responsible for the increase in the surface hydrophilicity of the membrane, the hydrophilicity would decrease if the consumption of hydroxyl groups for the crosslinking reaction between PVA and TEOS was higher than the generation of hydroxyl groups from

Applied Polymer SCIENCE

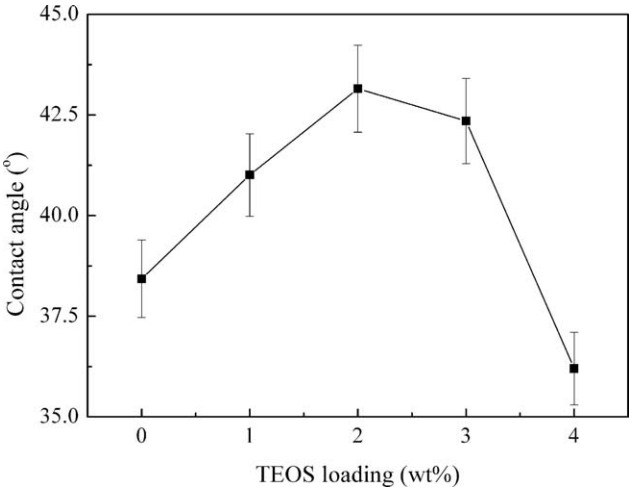

Figure 4. Effect of the TEOS loading on the contact angle of the PVA/TEOS membrane.

TEOS hydrolysis. On the contrary, the surface hydrophilicity of the membranes were thus strengthened.

The ε and the mean pore size values of the PVA/TEOS membranes with different TEOS loadings are listed in Table II. With increasing TEOS loading in the dope solution, both ε and r_m of the PVA/TEOS membrane increased. After the addition of the TEOS sol to the PVA aqueous solution, the crosslinking reaction occurred; this resulted in the higher combining force between SiO_2 and PVA and the possibly more compact structure during the formation of membrane.[37] However, the viscosity of the dope solution was reduced after the addition of the TEOS sol because of the water contained in the TEOS sol; therefore, the diffusion rate of the solvents in the coagulation bath increased during the precipitation process. This favored the formation of the larger pores; thus, ε and the pore size of the membranes increased.

Table II. Pore Structure Parameters of the PVA/TEOS Membranes

Membrane no.	ε (%)	r_m (nm)
M1	68.92	9.1
M2	70.15	11.7
M3	74.37	12.5
M4	80.25	12.8
M5	82.63	17.1

Effect of the TEOS Loading in a Dope Solution on the Morphology and Permeation Performance of the Membranes

Figure 5 shows the cross-sectional images of the PVA/TEOS membranes with different TEOS loadings. The SEM images indicated that the addition of the TEOS sol greatly influenced the PVA membrane structures. For membranes without TEOS or lower TEOS loadings, uniform and cellular-like pores formed in the cross section of the membranes. However, with increasing TEOS loading, a larger pore and a looser structure in the cross section of the membranes were formed. This result was in agreement with the pore structural analysis of the PVA/TEOS membranes in Table II. The viscosity of the dope solution decreased after the addition of the TEOS sol to the PVA solution; this favored an acceleration of the precipitation rate of the dope solution in the coagulation bath with a tendency toward the formation of large pores or macrovoids.[45,46] Macrovoids were initiated by the nucleation of the polymer-poor phase beneath the skin layer, and its growth relied on the rate difference between the inflow rate of nonsolvent to the dope solution and the outflow rate of the solvent to the coagulation bath. For membranes with higher TEOS loadings (especially M5), the TEOS sol enhanced the affinity between the dope solution and the coagulant medium so that phase separation occurred easily or the formation of the polymer-poor phase was faster. Thus larger pores or macrovoids formed. These macrovoids not only decreased R of the membranes but also weakened the

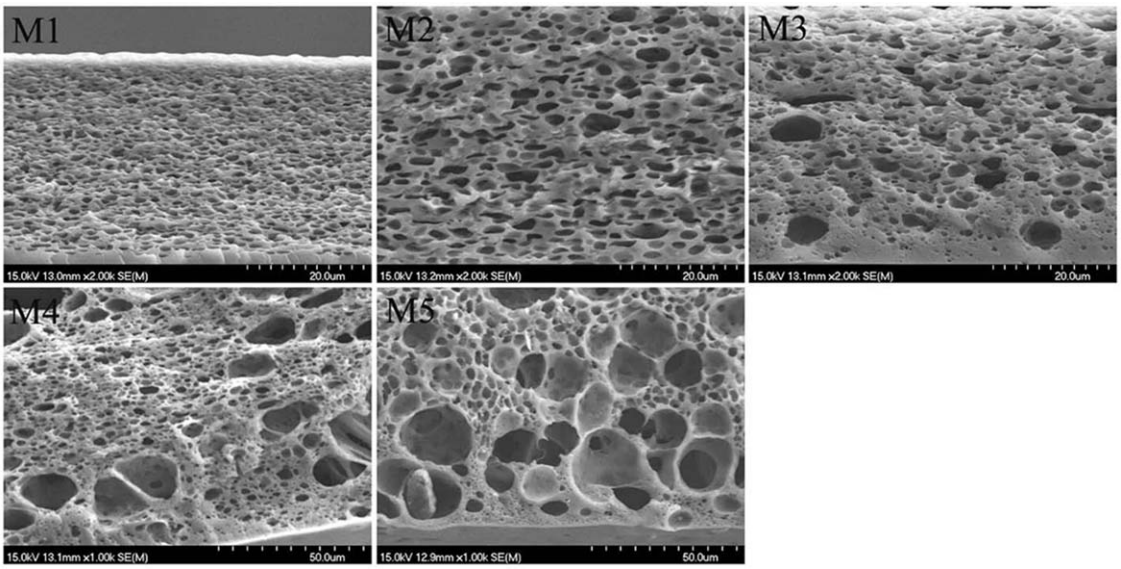

Figure 5. Cross-sectional images of the PVA/TEOS membranes with different TEOS loadings.

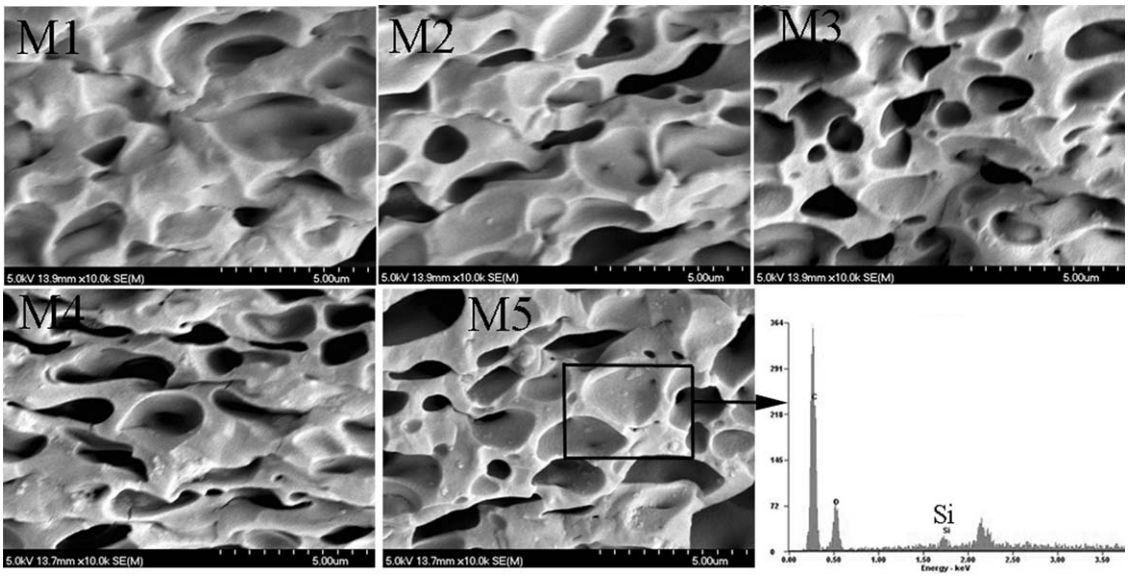

Figure 6. Magnified cross-sectional SEM images of the PVA/TEOS membranes.

mechanical properties. Therefore, it was not appropriate for the preparation of the PVA/TEOS UF membranes when the loading amount of TEOS was more than 3 wt %. As mentioned previously, the crosslinking frameworks formed in the PVA/TEOS membrane through Si—O—C covalent bonds and hydrogen bonds between the PVA and SiO_2 particles; this resulted in the homogeneous dispersal of SiO_2 particles in the PVA matrix. Therefore, the mechanical strength and flexibility of the PVA/TEOS membranes, especially those with low TEOS loadings, were better than those of the PVA membrane.

Figure 6 shows the magnified cross-sectional SEM images of the PVA/TEOS membranes with different TEOS loadings. As shown in Figure 6, there were no aggregates of SiO_2 particles in the PVA/TEOS membranes with low TEOS loadings; this meant that SiO_2 was homogeneously dispersed in the PVA matrix. However, some aggregates of SiO_2 particles were observed in the membrane with a higher TEOS loading (M5), and the average size of the SiO_2 particles was less than 50 nm; these aggregates formed the large pores or macrovoids around SiO_2 particles and led to a structural defect in the membrane. The presence of the SiO_2 particles was confirmed by energy-dispersive X-ray analysis, as shown in Figure 6. As reported in refs. 47 and 48, the size of SiO_2 particles with the same preparation method used in this study was about 7 nm, and the SiO_2 agglomerate size was about 50 nm. Therefore, the PVA/TEOS membranes with low TEOS loadings had the better pore structure; this was beneficial for the improvement of the permeation properties of the membranes.

The external surface morphologies of the PVA membrane with and without TEOS loadings are shown in Figure 7. The loaded TEOS membrane (M4) presented an increase in the surface pores compared with the PVA membrane (M1). The ratio of the coagulant medium inflow to solvent outflow was of the utmost importance to the structure of the external surface. If the coagulant medium diffused into the dope solution before the solvent in the dope solution desolvated into the coagulation bath, the coagulant medium may have created pores in the external surface of the membrane.[22] The decrease in the viscosity of the dope solution after the addition of the TEOS sol resulted in a faster coagulant medium inflow to the dope solution. On the other hand, the crosslinking reaction between PVA and TEOS restricted the outward diffusion of PVA, and these

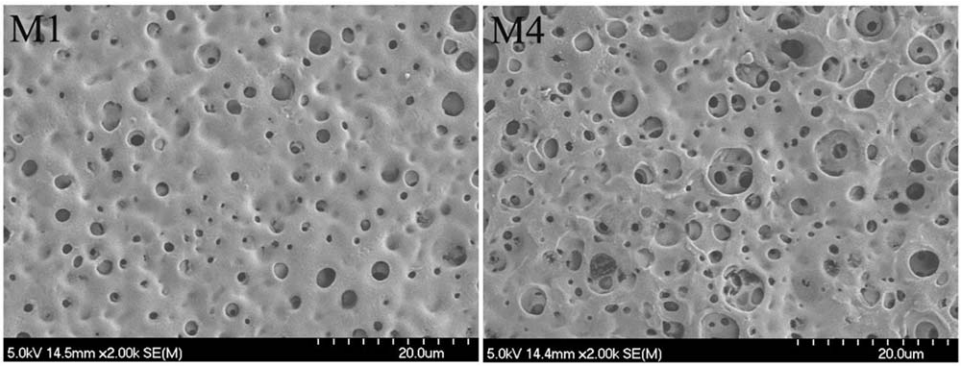

Figure 7. External surface morphologies of the M1 and M4 membranes.

Applied Polymer SCIENCE

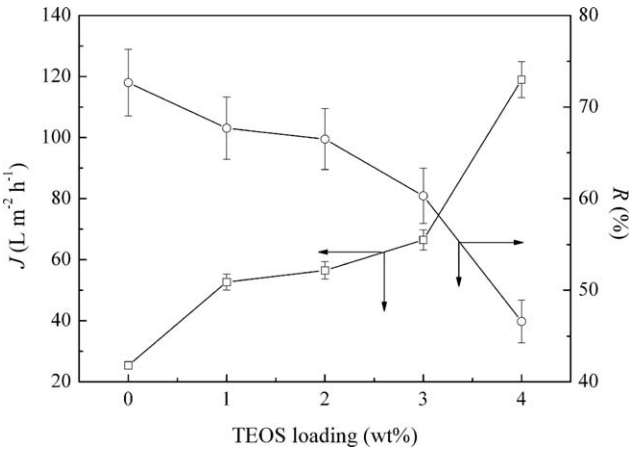

Figure 8. Effect of the TEOS loading in the dope solution on the permeation performance of the PVA/TEOS membrane.

tended to form the thin top layer and porous external surface of the membrane.

As mentioned previously, the structure of the PVA/TEOS membrane was influenced greatly by the TEOS loading; this thereby altered the permeation performance of the membranes. Figure 8 shows effect of the TEOS loading in the dope solution on the permeation performance of the PVA/TEOS UF membranes. As shown in Figure 8, with increasing TEOS loading, J_W increased, whereas the BSA R decreased; this was in accordance with the pore structure presented in Table II and the morphological analysis of the PVA/TEOS membranes.

Effect of the PEG Content on the Permeation Performance of the Membranes

To control the membrane structure, the low-molecular-weight component or the secondary polymer is frequently used as an additive in membrane forming system, which offers a convenient and effective way to develop membrane with high performances.[21,22] PEG is often used as the additive and the pore-forming agent in dope solution. Not only does it affect the precipitation rate of dope solution, but also the pore size and ε of membrane. The effect of PEG content in dope solution on the cross-sectional morphologies of PVA/TEOS membranes is shown in Figure 9. With increasing PEG content in the dope solution, the uniform cellular-like structural changed into one full of the larger pores or macrovoids, especially for the membranes with higher PEG contents (M8 and M9). PEG in the dope solution caused an enhancement in the precipitation rate,[49,50] and this improved the coagulant medium inflow to hasten the phase separation for generating the pore in the cross sections of the membranes. However, when excessive PEG was used, the PEG molecules could aggregate and, as a consequence, formed larger pores or macrovoids (M9). Nevertheless, after the PVA/TEOS membrane was formed, PEG was separated out continuously from the membrane when it was soaked in deionized water, thus, the pores in membrane formed sequentially.

Figure 10 shows the external surface images of the PVA/TEOS membranes with different PEG contents. With increasing PEG content in the dope solution, more and larger pores formed on the external surface of the membranes. The effect of PEG on the formation of pores in the external surface was attributed to the fact that water was a good solvent for PEG. As soon as the dope solution was immersed in the coagulation bath, PEG near the surface was dissolved in the coagulation bath; then the pores were generated on the membrane outer surface. In addition, PEG favored the phase separation of the dope solution in the coagulation bath. This reduced the solvent outflow in the dope solution and increased the coagulation medium inflow, and more and larger pores thus formed on the external surface of the membrane.

The effect of the PEG content on the permeation performance of the PVA/TEOS membranes is shown in Figure 11. The permeation performance was greatly affected by the PEG content in the dope solution. An increase in the PEG content appreciably increased J_W of the membrane but decreased BSA R. The

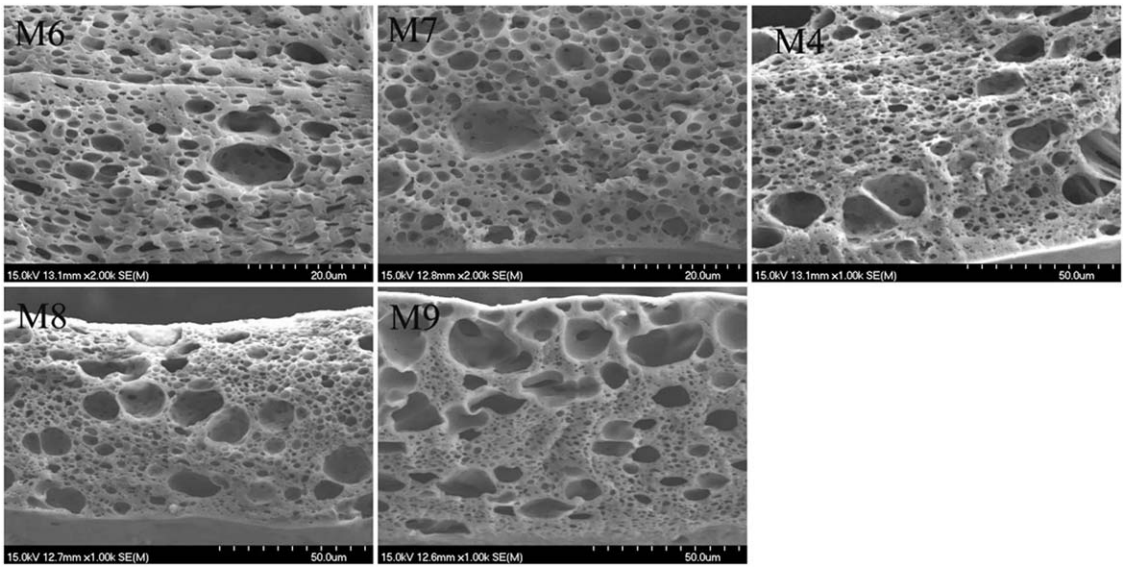

Figure 9. Cross-sectional images of the PVA/TEOS membranes with different PEG contents.

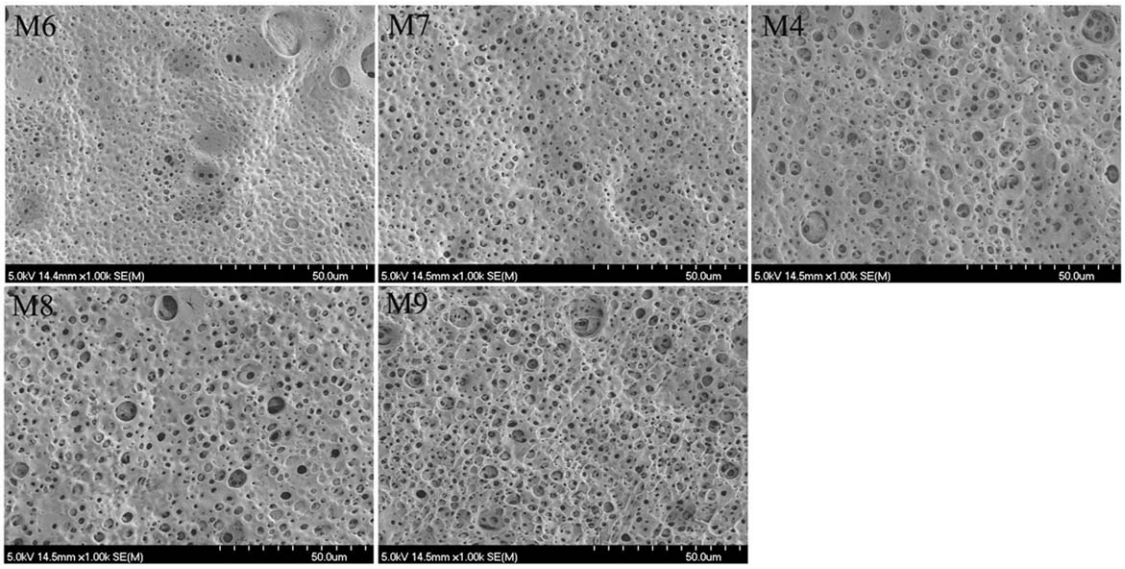

Figure 10. External surface images of the PVA/TEOS membranes with different PEG contents.

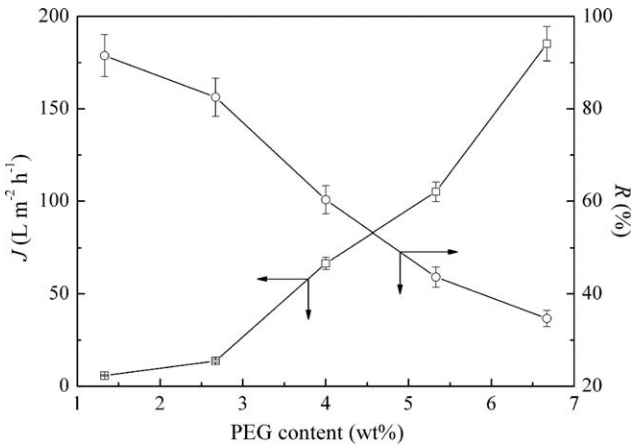

Figure 11. Effect of the PEG content on the permeation performance of the PVA/TEOS membrane.

results were consistent with the observations of the SEM images shown in Figures 9 and 10; this suggested that the PEG additives played an important role in the formation of more pores or even macrovoids in the cross section and on the outer surface of the membrane.

Antifouling Properties

A hydrophilic membrane possesses a high surface tension and has the ability to form hydrogen bonds with water, therefore, a water layer exists between the membrane and the bulk solution. The presence of this layer results in a reduced adhesion for foulants and effectively improves the antifouling properties; this is the main reason we chose PVA as a basic membrane material in this study. To provide long-term antifouling behaviors to the modified membranes, PVA and PVA/TEOS membranes were filtered with BSA aqueous solution and backwashed with water, and these cycle procedures were carried out three times. Table III shows a comparison of the antifouling properties between the PVA and PVA/TEOS UF membranes. After three cycles of filtration and backwashing, the R_r's of the PVA and PVA/TEOS membranes were both greater than 90%; this indicated that the PVA and PVA/TEOS UF membranes exhibited minimal protein adsorption potential and good long-term antifouling properties. Moreover, R_r of M4 was higher than that of M1; this suggested that the PVA/TEOS membrane had better antifouling properties than the PVA membrane. Compared with the PVA membrane, the PVA/TEOS membranes still retained a strong hydrophilicity, better mechanical strength, and lower water solubility; this endowed them with excellent antifouling properties. Therefore, the PVA/TEOS UF membranes had excellent cleanability and are a powerful alternative for fouling mitigation in practical applications.

CONCLUSIONS

Organic–inorganic PVA/TEOS hybrid UF membranes with a high water flux and good antifouling properties were prepared by the sol–gel method. The membrane was characterized by FTIR spectroscopy, XRD, static contact angle measurement, and SEM. The introduction of TEOS to PVA in preparing the PVA/

Table III. Comparison of the Antifouling Properties of the PVA and PVA/TEOS UF Membranes

Membrane no.	J_{W1} (L m^{-2} h^{-1})	J_{W2} (L m^{-2} h^{-1})	$(R_r)_{2/1}$	J_{W3} (L m^{-2} h^{-1})	$(R_r)_{3/1}$	J_{W4} (L m^{-2} h^{-1})	$(R_r)_{4/1}$
M1	25.4	24.5	96.49	23.9	94.09	23.5	92.52
M4	66.5	65.6	98.63	64.4	96.84	63.1	94.89

TEOS membranes made up for the poor intensity of the wet PVA membrane, and it still retained the strong hydrophilicity; this helped the membrane achieve the required performance in the membrane with a controllable structure and antifouling behaviors. The effects of the TEOS loading and PEG content in the dope solution on the morphologies, J_W values, and BSA R values of the PVA/TEOS membranes were investigated. J_W of the membrane increased with increasing TEOS loading and PEG content, whereas BSA R declined. In addition, the filtration and backwashing experiment showed that the PVA/TEOS UF membrane had excellent long-term antifouling properties to protein.

ACKNOWLEDGMENTS

The authors gratefully acknowledge the National Natural Science Foundation of China (contract grant number 21206146) for its financial supports of this project.

REFERENCES

1. Afonso, M. D.; Borquez, R. *Desalination* **2002**, *142*, 29.
2. Bruggen, B. V.; Vandecasteele, C.; Gestel, T. V.; Doyen, W.; Leysen, R. *Environ. Prog.* **2003**, *22*, 46.
3. Vadavyasan, C. V. *Desalination* **2007**, *203*, 296.
4. Goosen, M. F. A.; Sablani, S. S.; Ai-Hinai, H.; Ai-Obeidani, S.; Al-Belushi, R.; Jackson, D. *Sep. Sci. Technol.* **2004**, *39*, 2261.
5. Ma, X. L.; Su, Y. L.; Sun, Q.; Wang, Y. Q.; Jiang, Z. Y. *J. Membr. Sci.* **2007**, *300*, 71.
6. Du, R. J.; Peldszus, S.; Huck, P. M.; Feng, X. S. *Water Res.* **2009**, *43*, 4559.
7. Nguyen, A. H.; Narbaitz, R. M.; Matsuura, T. *J. Environ. Eng. ASCE* **2007**, *133*, 515.
8. Wavhal, D. S.; Fisher, E. R. *Langmuir* **2003**, *19*, 79.
9. Kou, R. Q.; Xu, Z. K.; Deng, H. T.; Liu, Z. M.; Seta, P.; Xu, Y. *Langmuir* **2003**, *19*, 6869.
10. Wang, X. F.; Chen, X. M.; Yoon, K.; Fang, D. F.; Hsiao, B. S.; Chu, B. *Environ. Sci. Technol.* **2005**, *39*, 7684.
11. Ma, H. Y.; Yong, K. W.; Rong, L. X.; Shokralla, M.; Kopot, A.; Wang, X.; Fang, D. F.; Hsiao, B. S.; Chu, B. *Ind. Eng. Chem. Res.* **2010**, *49*, 11978.
12. Wang, X. F.; Fang, D. F.; Yoon, K.; Hsiao, B. S.; Chu, B. *J. Membr. Sci.* **2006**, *278*, 261.
13. Asatekin, A.; Kang, S.; Elimelech, M.; Mayes, A. M. *J. Membr. Sci.* **2007**, *298*, 136.
14. Park, J. Y.; Acar, M. H.; Akthakul, A.; Kuhlman, W.; Mayes, A. M. *Biomaterials* **2006**, *27*, 856.
15. Amanda, A.; Kulprathipanja, A.; Toennesen, M.; Mallapragada, S. K. *J. Membr. Sci.* **2000**, *176*, 87.
16. Gudeman, L. F.; Peppas, N. A. *J. Appl. Polym. Sci.* **1995**, *55*, 919.
17. Hu, W. W.; Zhang, X. H.; Zhang, Q. G.; Liu, Q. L.; Zhu, A. M. *J. Appl. Polym. Sci.* **2012**, *126*, 778.
18. Jahanshahi, M.; Rahimpour, A.; Peyravi, M. *Desalination* **2010**, *257*, 129.
19. Kang, G. D.; Cao, Y. M. *Water Res.* **2012**, *46*, 584.
20. Song, Y. J.; Liu, F.; Sun, B. H. *J. Appl. Polym. Sci.* **2005**, *95*, 1251.
21. Chuang, W. Y.; Young, T. H.; Chiu, W. Y. *J. Membr. Sci.* **2000**, *172*, 241.
22. Chuang, W. Y.; Young, T. H.; Chiu, W. Y.; Lin, C. Y. *Polymer* **2000**, *41*, 5633.
23. Burezack, K.; Fujisato, T.; Hatada, M.; Ikada, Y. *Biomaterials* **1994**, *15*, 231.
24. Liu, S. X.; Kim, J. T.; Kim, S. *J. Food Sci.* **2008**, *73*, 143.
25. Shang, Y.; Peng, Y. L. *Desalination* **2008**, *221*, 324.
26. Lu, X. F.; Bian, X. K.; Shi, L. Q. *J. Membr. Sci.* **2002**, *210*, 3.
27. Zhang, Y. Z.; Li, H. Q.; Li, H.; Li, R.; Xiao, C. F. *Desalination* **2006**, *192*, 214.
28. Cho, J. W.; Sul, K. I. *Polymer* **2001**, *42*, 727.
29. Zoppi, R. A.; Soares, C. G. A. *Adv. Polym. Technol.* **2002**, *21*, 2.
30. Jiang, Y. P.; Wang, R. S. *Chem. Eng. (China)* **2003**, *31*, 38.
31. Jiang, Y. P.; Wang, R. S. *Polym. Mater. Sci. Eng. (China)* **2002**, *18*, 177.
32. Li, J. F.; Xu, Z. L.; Yang, H. *Polym. Adv. Technol.* **2008**, *19*, 251.
33. Yu, L. Y.; Shen, H. M.; Xu, Z. L. *J. Appl. Polym. Sci.* **2009**, *113*, 1763.
34. Feng, C. S.; Shi, B. L.; Li, G. M.; Wu, Y. L. *J. Membr. Sci.* **2004**, *237*, 15.
35. Yang, C. C.; Lin, S. *J. Mater. Lett.* **2002**, *57*, 873.
36. Yang, C. C.; Lin, S. J. *J. Appl. Electrochem.* **2003**, *33*, 777.
37. Kariduraganavar, M. Y.; Kulkarni, S. S.; Kittur, A. A. *J. Membr. Sci.* **2005**, *246*, 83.
38. Zhang, Q. G.; Liu, Q. L.; Chen, Y.; Chen, J. H. *Ind. Eng. Chem. Res.* **2007**, *46*, 913.
39. Xue, X. M.; Li, F. T. *Micropor. Mesopor. Mater.* **2008**, *116*, 116.
40. Peppas, N. A.; Wright, L. *Macromolecules* **1996**, *29*, 8798.
41. Hennink, W. E.; Nostrum, C. F. *Adv. Drug Delivery Rev.* **2002**, *54*, 13.
42. Peppas, N. A. *Macromol. Chem.* **1977**, *178*, 595.
43. Wang, Y. L.; Yang, H.; Xu, Z. L. *J. Appl. Polym. Sci.* **2008**, *107*, 1423.
44. Yang, Y. N.; Wang, P. *Polymer* **2006**, *47*, 2683.
45. Mulder, M. Basic Principles of Membrane Technology; Kluwer Academic: Dordrecht, The Netherlands, **1991**.
46. Lin, F. C.; Wang, D. M.; Lai, C. L.; Lai, J. Y. *J. Membr. Sci.* **1997**, *123*, 281.
47. Rio, C.; Jurado, J. R.; Acosta, J. L. *Polymer* **2005**, *46*, 3975.
48. Kim, Y. M.; Choi, S. H.; Lee, H. C.; Hong, M. Z.; Kim, K.; Lee, H. I. *Electrochim. Acta* **2004**, *49*, 4787.
49. Young, T. H.; Chuang, W. Y.; Yao, N. K.; Chen, L. W. *J. Biomed. Mater. Res* **1998**, *40*, 385.
50. Young, T. H.; Yao, N. K.; Chang, R. F.; Chen, L. W. *Biomaterials* **1996**, *17*, 2139.